Inverse photoemission with energy resolution better than 200 meV

M. Budke,[1] V. Renken,[1] H. Liebl,[2,3] G. Rangelov,[1] and M. Donath[1]
[1] *Physikalisches Institut, Westfälische Wilhelms-Universität Münster, Wilhelm-Klemm-Str. 10, 48149 Münster, Germany*
[2] *Hartstr. 17, 85386 Eching, Germany*
[3] *Max-Planck-Institut für Plasmaphysik, EURATOM Association, 85740 Garching bei München, Germany*
(Dated: March 7, 2008)

We present a spectrometer for inverse photoemission in the VUV range with variable energy resolution between 400 and 165 meV FWHM (full width at half maximum). The energy distribution of the electron beam used for excitation can be adjusted between 300 and 125 meV by the use of a toroidal 90° electrostatic deflector combined with a slit aperture. The emitted photons are detected by Geiger-Müller counters filled with either acetone or iodine as counting gas. The optical bandpasses of the detectors can be tuned between 100 and 330 meV by varying the temperature of their entrance windows. The overall resolution of the spectrometer is determined by measuring the Fermi-level onset in inverse-photoemission data of polycrystalline gold. Furthermore, the resolution enhancement is demonstrated by spectra of image-potential-induced surface states at Cu(001).

I. INTRODUCTION

Angle-resolved photoemission (PE)[1–3] and inverse photoemission (IPE)[4–6] are two complementary methods for probing the electronic structure of solid surfaces below and above the Fermi level E_F. By adding spin analysis of the emitted electrons in PE or by the use of a spin-polarized electron beam for excitation in IPE, extra information about the spin dependence of their electronic structure is obtained.

In state-of-the-art set-ups for photoemission, the achievable energy resolution is well below 10 meV. With spin-resolved detection, however, the energy resolution is typically reduced by about one order of magnitude. This is caused by the intensity loss of 3 to 4 orders of magnitude in the spin detector, which requires a trade-off between intensity (reasonable measuring time) and energy resolution. In inverse photoemission a compromise between energy resolution and measuring time has to be accepted as well. Since the cross section for the IPE process in the VUV range is about 5 orders of magnitude smaller than for photoemission,[7] IPE generally suffers from very low counting rates. Therefore, special attention has to be given to high-performance electron guns with currents in the μA range and to photon detectors with high sensitivity. It should be noted that using spin-polarized electrons causes no further intensity loss in IPE.

As electron source for spin-integrated IPE measurements thermal emitters like tungsten or barium-oxide cathodes are used. The latter provide a better resolution because they operate at lower temperatures (1100 K).[8] Typical energy resolutions achievable with these cathodes are between 300 and 500 meV (FWHM). For spin-resolved IPE measurements, mostly GaAs photoemitters are used with an energy spread of around 300 meV, depending on the current being extracted from the cathode.[9–11] Fortunately, they provide emission currents comparable with conventional electron guns at similar or slightly better resolution.

The photons being emitted in the IPE process are detected by grating monochromators combined with photomultipliers or by bandpass detectors of various types, e.g., Geiger-Müller counters or solid-state detectors. The former offer variable photon energies and good energy resolution of about 100 meV but have a lower sensitivity compared with the latter that are restricted to one detection energy only. The optical bandpass of the Geiger-Müller counter is provided by the ionization threshold of the counting gas on the low-energy side and the transmission cut-off of the entrance window on the high-energy side. IPE in the VUV range started with this type of detector.[12] With iodine as counting gas and CaF_2 as entrance window this detector achieves an energy resolution of about 700 meV. The resolution can be improved to 270 meV by using SrF_2 as entrance window.[13] The width of the optical bandpass can be further reduced to about 170 meV by heating the SrF_2,[14,15] which shifts the transmission cutoff to lower energy.[16,17] In this case, the SrF_2 window has to be used in addition to the necessary entrance window of the counter. It must be mounted thermally isolated from the counter because the counting efficiency depends strongly on the temperature-dependent pressure of the counting gas.[18]

Over the years, various gas/window combinations for use in energy-selective Geiger-Müller counters have been proposed.[19–22] Acetone vapour in combination with a CaF_2 window provides an optical resolution of about 400 meV (FWHM) at almost the same sensitivity as the iodine-filled counter.[19] Compared with iodine, acetone turned out to be much easier to handle with respect to corrosion of the stainless steel tube leading to regular leakage problems at the sealing surfaces in the case of iodine. Recently, the energy resolution of an acetone-filled

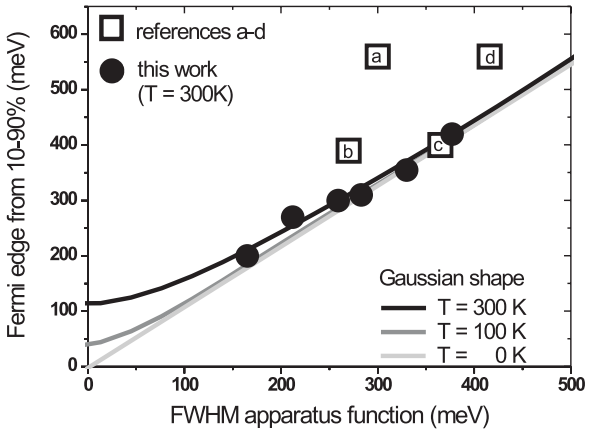

FIG. 1: Relation between the rise from 10 to 90% of the IPE signal at the Fermi edge and the FWHM of the apparatus function. Lines are calculations for Fermi distributions at different temperatures convoluted with Gaussian-shaped apparatus functions. Dots represent results for various operating conditions of our spectrometer, squares are taken from different experiments in the literature (a[23], b[24], c[14], d[21]).

counter could be significantly improved to 115 meV by adding an oxygen or krypton gas absorption filter.[22]

Up to now, all efforts of improving the energy resolution in IPE concentrated on the photon detector. The total resolution of an IPE spectrometer, however, is given by the convolution of the optical bandpass and the electron energy distribution. Provided that these contributions can be described by functions with $\sigma^2_{\rm opt}$ and $\sigma^2_{\rm el}$ being their variances, the total energy resolution has a variance of

$$\sigma^2_{\rm tot} = \sigma^2_{\rm opt} + \sigma^2_{\rm el},$$

corresponding in the case of Gaussian functions to a FWHM of

$$\mathrm{FWHM} = 2\sigma_{\rm tot}\sqrt{2ln2}.$$

As discussed above, the resolution of conventional electron sources is limited to about 300 meV. Hence it is obvious that, for further improvement of the total energy resolution, one must reduce the width of the electron energy distribution as well.

The term 'resolution' is not a well-defined quantity in the literature. The FWHM is a good measure of the quality of an apparatus function but also its shape is crucial for comparability between apparatus functions of different spectrometers. Two spectrometers with the same FWHM of their apparatus functions may still have different resolutions. A stronger criterion for the resolution than the FWHM is the rise of the IPE signal at the Fermi edge from 10 to 90%. In Figure 1, the relation between the 10-90% criterion and the FWHM is demonstrated for theoretical apparatus functions with Gaussian shape and several experimental apparatus functions. The values for the theoretical 10-90% widths are obtained by convoluting the Fermi distribution function for 0 K (light grey line), 100 K (dark grey line) and 300 K (black line) with Gaussians of given FWHM. Note that the energetic width between 10% and 90% of the intensity rise at the Fermi level is limited by the Fermi distribution at finite temperature. Therefore, the relation between the 10-90% width and the FWHM for a Gaussian-shaped apparatus function gives a straight line only for T=0 (light grey line in Fig. 1). For a given experimental apparatus function, one can determine both values, the 10-90% width and the FWHM and plot the result in the diagram of Fig. 1. Data points above the calculated lines indicate apparatus functions which have longer 'tails' than a Gaussian function, data points below represent apparatus functions that are narrower than a Gaussian. We have tested four experimental apparatus functions from the literature and have included the results as open squares in Fig. 1. Three data points lie significantly above, one on top of the 'Gaussian line'. The results of our work are included as filled dots and will be described in this paper. A further issue should be noted: several apparatus functions reported in the literature are not symmetric with the consequence that the spectral features including the Fermi-level onset are asymmetric as well.

In this paper we present a spectrometer for inverse photoemission with variable energy resolution. This has the advantage that the IPE spectra can be measured at an energy resolution as good as necessary with an intensity as high as possible. Our electron gun emits an electron beam with an almost Gaussian-shaped energy distribution of tunable width. Two Geiger-Müller counters filled with acetone and iodine, respectively, are compared regarding energy resolution, sensitivity and manageability. MgF_2 is used as entrance window, combined with an additional window of CaF_2 or SrF_2, whose temperature can be varied for tuning the optical resolution. The total energy resolution of our spectrometer is determined by measuring the Fermi edge of polycrystalline gold and finally the resolution enhancement is demonstrated for image-potential-induced surface states on Cu(100).

II. ELECTRON SOURCE

Our IPE system can be operated with different electron sources: a BaO cathode for spin-integrated and a GaAs photocathode for spin-resolved measurements. The BaO cathode is a commercially available cathode that is indirectly heated to its operating temperature of about 1100 K. The design of the spin-polarized electron source based on a GaAs photocathode is very similar to the one described in the literature.[10] The key difference is the use of a 90° toroidal instead of a spherical electrostatic deflector and an additional 1.5 mm slit aperture at the focal

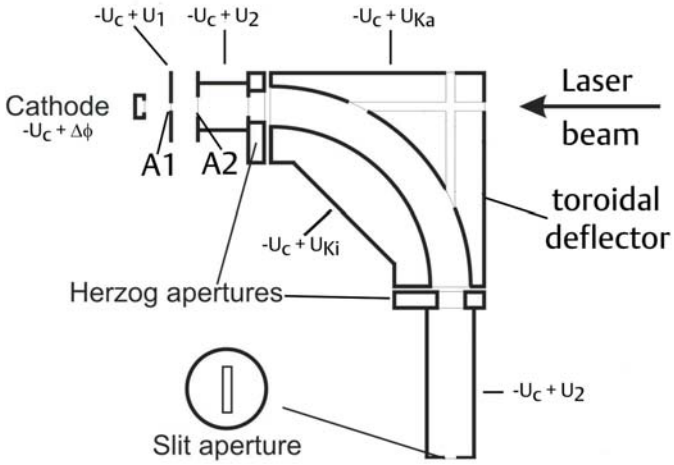

FIG. 2: Schematics of the energy-dispersive part of the electron optics.

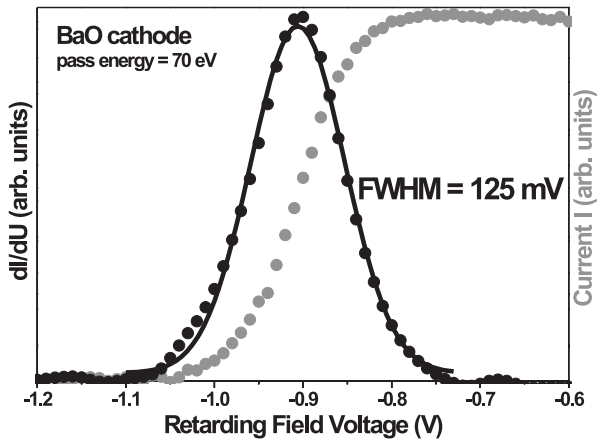

FIG. 3: Electron energy distribution obtained in the LEM at a pass energy of 70 eV: integrated electron energy distribution as measured by a retarding field analyser (grey dots), electron energy distribution (black dots) and fit to the data by a Gaussian function (black line).

point of the deflector exit. As a consequence, the deflector is not only used for changing the spin polarization of the electrons relative to their propagation direction but also for reducing the width of their energy distribution depending on the chosen pass energy.

If the pass energy of the deflector is set to 500 eV as in the original design,[10] called *high-energy mode* (HEM), about 80% of the emitted electrons are transferred to the sample via an electron optics with an energy distribution of about 300 meV (FWHM). In the *low-energy mode* (LEM), the pass energy of the deflector is reduced to 200 eV and lower which leads to a higher energy resolution at the cost of the transmitted current. The choice of the pass energy allows IPE measurements either with high energy resolution or with high electron current, adjustable to the physics problem to be solved. For example, at a pass energy of 70 eV, the FWHM of the electron energy distribution behind the slit is reduced to 125 meV combined with a reduction of the transmitted current by a factor of 5.

In the following, we will explain the modifications of the deflector in detail as shown in Fig. 2. After leaving the cathode held at a potential of $-U_c+\Delta\Phi$ the electrons pass two apertures, A1 and A2, the latter being at a potential that defines the pass energy of the deflector. To obtain the correct pass energy, the difference $\Delta\Phi$ between the work functions of the cathode and the electron optics must be considered. In the HEM both apertures are at a potential of 500 V with respect to U_c while in the LEM the voltage U_1 is about three times higher than U_2. In combination with the cathode these two apertures form a three-electrode emission lens.[25] After passing the aperture A2, the electrons enter the deflector, which maps an image of the emission spot, modified by the emission lens, onto the slit aperture. Caused by the finite energy distribution, this image is elongated in the direction of energy disperion so that the slit aperture cuts out a part of the electron beam. As a consequence, the width of the energy distribution of the transmitted electrons is reduced. To improve the energy-dispersive properties, the spherical deflector used in our former design[10] was replaced by a toroidal geometry. By choosing the toroidal geometry, the transversal aperture error, corresponding to the direction of energy dispersion of the deflector, is much smaller than in a spherical geometry.[26] After passing the slit aperture the electrons enter the transfer part of the electron optics, which is identical to our former design.[10]

The electron beam is characterized by use of a Faraday cup mounted on a xyz manipulator at the position where the sample is usually located. The electrons enter the Faraday cup through a circular aperture (0.5 mm in diameter) and pass two grids, congruently arranged in a distance of 0.9 mm, before being collected. By applying a retarding field voltage to the two grids the (integrated) energy distribution of the electrons can be determined. Since the energy resolution of a retarding field analyser is proportional to the energy of the incident electrons,[27] we used a low kinetic energy of 0.9 eV. In this case, the resolution of our analyser is below 0.02 eV and can therefore be neglected in our analysis.

The integrated energy distribution of the electron beam was determined by measuring the Faraday-cup current as a function of the retarding field voltage. Figure 3 presents as grey dots a result for a pass energy of 70 eV and a total sample current of 0.5 μA from the BaO cathode. The latter was measured on the outer part of the Faraday cup.

To obtain the energy distribution of the electrons, the data have to be differentiated. Numerically, this has been

done by convoluting the measured data with a differentiated Gaussian function with a variance of $(10\ \mathrm{meV})^2$. According to the convolution theorem, this corresponds to a differentiation of the data that has been convoluted with a Gaussian before. So in addition to differentiation, there is also a smoothing effect, which, in our case, is negligible in comparison with the width of the distribution. The result is shown in Fig. 3 as black dots and is well described by a Gaussian with a FWHM of 125 meV (black line). This states an improvement of more than a factor of two compared with the former electron optics.[10]

III. PHOTON DETECTOR

The photon detector used in our IPE experiment is a standard Geiger-Müller counter with a MgF_2 entrance window (transmission cutoff at 10.9 eV). A detailed description of our basic design can be found in the literature.[28]

In our design, we added a copper carousel holding a CaF_2 and a SrF_2 window. Depending on the window material placed in front of the counter, the high-energy cutoff of the optical band pass is either 10.2 eV for CaF_2 or 9.69 eV for SrF_2.[29] The temperature of these extra windows can be varied between 77 and 400 K by pumping liquid nitrogen or hot air through stainless steel capillaries connected to the Cu element. Heating of the windows shifts their transmission cutoff to lower energy,[16,17] cooling has the opposite effect: the transmission cutoff shifts to higher energy.

We use acetone[19] as counting gas and compare the detector with an iodine-filled counter[12]. The photoionisation threshold of acetone is 9.69 eV[30] (9.23 eV for iodine[31]). Combined with a CaF_2 window at room temperature, the width of the optical band pass of the acetone-filled counter is expected to be about 400 meV.

Figure 4 presents the optical bandpass of our counter (black dots), measured with a VUV light source and a monochromator built by R. Stiepel.[22] The solid line shows the best fit to the data by a Gaussian function with 330 meV FWHM. In addition, Fig. 4 displays the scenarios for an acetone-filled counter either with a heated CaF_2 or a cooled SrF_2 window. Since heating of the entrance window shifts the transmission cutoff to lower energy, a significantly smaller width of the band pass is expected for a counter with heated CaF_2 window. Note that the mean detection energy shifts to lower energy as well. Using SrF_2 at room temperature as entrance window would provide a 'zero optical band pass'. Cooling the SrF_2 window gradually opens the optical band pass. In this arrangement, the energy resolution of the counter is, in principle, only limited by the desired sensitivity, which is directly connected with the width of the optical band pass.

The Geiger-Müller counter is pumped with a rotary pump, an oil trap and a turbo molecular pump to a pressure of less than 5×10^{-4} mbar. To fill the counter, first

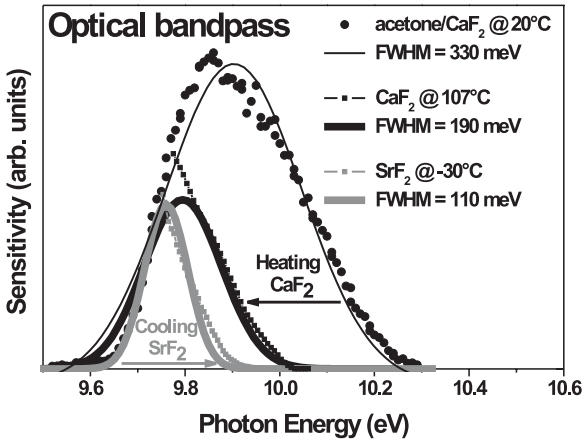

FIG. 4: Optical bandpass of the acetone/CaF_2 Geiger-Müller counter: data (black dots) and comparison with a Gaussian function of 330 meV FWHM (thin black line). The black and grey squares show schematically the cutoff of a heated CaF_2 window and of a cooled SrF_2 window, respectively. The associated optical bandpasses are shown as thick black and grey lines.

acetone vapour is let in to a partial pressure of 1 mbar as measured by a Pirani pressure transmitter. Then, argon as an amplification gas is let in to a total pressure of 200 mbar. The voltage applied to the counting wire is about 1000 V.

IV. OVERALL APPARATUS FUNCTION

We determined the total energy resolution of our IPE system by measuring the Fermi edge of a polycrystalline gold sample. The sample was cleaned by Ar ion bombardment and annealing to 600°C. For these measurements we used the BaO cathode and the LEM of the electron optics. At a pass energy of 70 eV, the optics provided a sample current of about 0.5 μA. We used both acetone and iodine-filled counters under otherwise equivalent conditions to compare their performance directly.

The results of the measurements are shown in Fig. 5. The dots represent the measured data and the lines are simulations fitted to the data. In these simulations we assume that the intrinsic signal $I(E)$ can be described by

$$I(E) = (a + bE) \times (1 - F(E)),$$

where $F(E)$ is the Fermi function at room temperature, b is the slope of a linear increasing background that was found in all measurements and a is a constant offset. The latter represents the almost constant density of states of

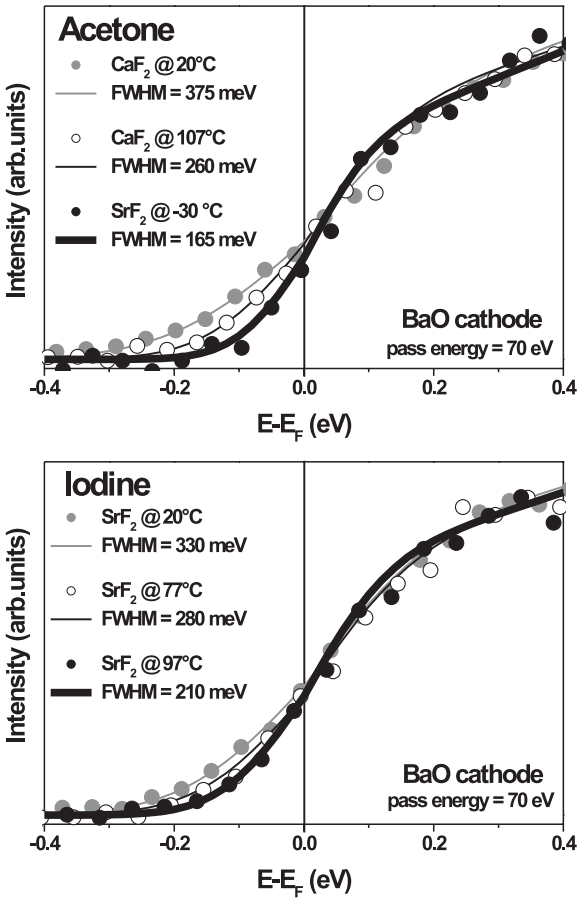

FIG. 5: Fermi edge of polycrystalline gold measured with a) the acetone-filled and b) the iodine-filled Geiger-Müller counter. Dots represent the measured data at different counter configurations. The lines are simulations fitted to the data to estimate the total energy resolution of the IPE spectrometer. Fit parameter is the FWHM of Gaussian-shaped apparatus functions (see text for details).

a free-electron metal close to the Fermi level. In the simulations, $I(E)$ is convoluted with Gaussians of different FWHM until good agreement with the experiment is reached. Thus, the FWHM of the Gaussian giving best agreement between simulation and experiment is a good estimate of the overall apparatus function, i.e., the total experimental resolution.

The combination of acetone as counting gas and CaF_2 as entrance window results in an apparatus function with FWHM of 375 meV (grey line in Fig. 5a). The width of the optical band pass was determined to 330 meV (Fig. 4), so the width of the electron energy distribution is calculated to be 180 meV in this experiment. Note, that this value is higher than in Fig. 3 and in the following experiments. The electron energy distribution depends primarily on the pass energy but also on the beam current (space charge effects within the electron optics) and on the specific settings of the electron optics. When the entrance window is heated to a temperature of 107°C, the measured Fermi edge is much sharper and represents a total energy resolution of 260 meV (thin black line). We achieved the best energy resolution with SrF_2 at −30°C as entrance window. The simulation (thick black line) indicates a width of the apparatus function of only 165 meV (FWHM). This value is about a factor of 2 smaller than the best energy resolution reported for IPE systems so far[24].

The use of iodine as counting gas combined with a SrF_2 window at 20°C provides a Fermi edge that indicates a resolution of 330 meV (grey line in Fig. 5b). This is significantly sharper than the results achieved with the combination acetone/CaF_2 (20°C). When the entrance window is heated to 77 and 97°C, the resolution is improved to 280 and 210 meV, respectively (thin and thick black lines in Fig. 5b).

In Figure 1, we had characterized experimental IPE apparatus functions by two criteria, the FWHM and the 10-90% increase of the Fermi-level onset. We have included the results for our detector with different gas/window combinations as black dots in Fig. 1. The data points lie on top of the calculated lines, indicating that our apparatus functions are well described by Gaussian functions with no 'tails' in onset or decay.

The counting rates obtained with the iodine-filled counter were about 30% higher compared with the acetone-filled counter under otherwise identical conditions. At 0.8 eV above the Fermi edge typical counting rates with an unheated SrF_2 window were around 11 Counts/μAs and decreased to 3 Counts/μAs as the window was heated to 97°C. The dark count rate created by background radiation was between 0.05 Hz and 0.1 Hz in all experiments.

To demonstrate the improved energy resolution of our IPE spectrometer, we performed measurements on the image-potential-induced surface states of Cu(001)[32,33]. These states form a Rydberg-like series within less than one eV below the vacuum energy E_{vac} with binding energies of 0.57 eV, 0.18 eV and 0.08 eV for the first three members of the series. Their lifetimes have been determined in a two-photon photoemission experiment to 40 fs, 110 fs, and 300 fs for the $n = 1$, 2, and 3 states, respectively.[34] This corresponds to lifetime-induced linewidths of 16.5 meV, 6 meV and 2.2 meV. An energy-resolved two-photon photoemission experiment obtained a linewidth of 28 meV for the $n = 1$ state[35] which is significantly smaller than the apparatus function in IPE. Therefore, the appearance of image states in IPE is dominated by the apparatus function.

The Cu(001) sample was cleaned in a standard procedure by 1000 eV Ar ion bombardment and annealing to 650°C. We used the GaAs photocathode as electron source with a pass energy of 55 eV of the deflector. The sample current was between 1.5 μA and 2 μA. As pho-

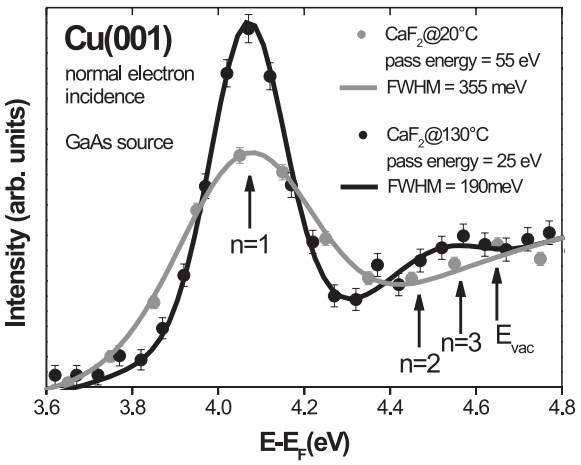

FIG. 6: Image-potential states of Cu(001) measured with two different experimental resolutions. Grey dots (black dots) denote a measurement with a deflector pass energy of 55 eV (25 eV) and a temperature of 20°C (130°C) for the CaF_2 window in front of the acetone-filled Geiger-Müller counter. The lines are simulations to determine the widths of the apparatus functions (see text for details).

ton detector we used the acetone counter in combination with CaF_2 at 20°C as entrance window. The grey dots in Fig. 6 show our IPE data of the image states for normal electron incidence. To estimate the width of the apparatus function we performed a model calculation taking into account the first three members of the image-state series and the continuum states starting at $E_{\rm vac}$ simulated by a step-like increase.[36] Additionally, we added a linear increase to simulate the IPE background. To model the influence of the apparatus function, the result was convoluted with Gaussians of different FWHM until good agreement with the measured data was achieved. The best fit is shown as grey line in Fig. 6, indicating a total energy resolution of the spectrometer of 355 meV. The total measuring time for the spectrum was about 15 minutes.

The black dots in Fig. 6 show an IPE measurement with improved energy resolution. The pass energy of the deflector was reduced to 25 eV and the entrance window of the counter was heated to 130°C. The linewidth of the $n = 1$ state is significantly reduced and the higher members of the series start to appear as a separate peak. The total energy resolution of the spectrometer as deduced from the simulation (black line) is about 190 meV. However, we had to pay a price for it. The measuring time had to be increased to several hours because the sample current and the detector sensitivity were both reduced by a factor of about 4.

V. SUMMARY

In this paper, we presented a spectrometer for inverse photoemission with variable energy resolution from 400 meV to 165 meV (FWHM). The latter value is an improvement of almost a factor of two compared with the best resolutions reported for IPE spectrometers so far. This significant improvement was only achieved by a resolution enhancement of the photon detector in combination with a decrease of the electron energy distribution used for excitation. Our studies on Geiger-Müller detectors with different combinations of counting gases and window materials show that acetone is an excellent alternative for the corrosive iodine.

Beside its superior energy resolution, the main advantage of our spectrometer is that it can be tuned to highest intensity for a desired energy resolution. Depending on the physics question to be solved, the operator can choose, within the described limits, between either a short measuring time und a limited energy resolution or a longer measuring time and a higher energy resolution.

Acknowledgments

We would like to thank R. Stiepel and C. Eibl for their help with measuring the optical bandpass of the acetone counter. We are indebted to C. Benesch, V. Dose, H. Merz, and D.H. Yu for helpful discussions.

[1] S. D. Kevan (Ed.), *Angle-Resolved Photoemission*, (Elsevier, Amsterdam, 1992).
[2] P. D. Johnson, Rep. Prog. Phys. **60**, 1217 (1997).
[3] S. Hüfner, *Photoelectron Spectroscopy, Principles and Applications*, (Springer, New York, 2003).
[4] V. Dose, Surf. Sci. Rep. **5**, 337 (1985).
[5] N. V. Smith, Rep. Prog. Phys. **51**, 1227 (1988).
[6] M. Donath, Surf. Sci. Rep. **20**, 251 (1994).
[7] J. B. Pendry, Phys. Rev. Lett. **45**, 1356 (1980).
[8] R. D. Young, Phys. Rev. **113**, 110 (1959).
[9] D. T. Pierce and F. Meier, Phys. Rev. B **13**, 5484 (1976).
[10] U. Kolac, M. Donath, K. Ertl, H. Liebl, and V. Dose, Rev. Sci. Instrum. **59**, 1933 (1988).
[11] M. Cantoni and R. Bertacco, Rev. Sci. Instrum. **75**, 2387 (2004).
[12] V. Dose, Appl. Phys. **14**, 117 (1977).
[13] A. Goldmann, M. Donath, W. Altmann, and V. Dose, Phys. Rev. B **32**, 837 (1985).
[14] V. Dose, Th. Fauster, and R. Schneider, Appl. Phys. A **40**, 203 (1986).
[15] J. Braun, C. Math, A. Postnikov, and M. Donath, Phys. Rev. B **65**, 184412 (2002).
[16] W. R. Hunter and S. A. Malo, Phys. Chem. Solids **30**, 2739 (1969).

[17] M. H. Reilly, J. Phys. Chem. Solids **31**, 1041 (1970).
[18] V. Dose, Rev. Sci. Instrum. **37**, 1055 (1968).
[19] D. Funnemann and H. Merz, J. Phys. E: Sci. Instrum. **19**, 554 (1986).
[20] P. M. G. Allen and P. J. Dobson, Solid State Commun. **55**, 701 (1987).
[21] J. A. Lipton-Duffin, A. G. Mark, and A. B. McLean, Rev. Sci. Instrum. **73**, 3149 (2002).
[22] R. Stiepel, R. Ostendorf, C. Benesch, and H. Zacharias, Rev. Sci. Instrum. **76**, 063109 (2005).
[23] M. Nakatake, Y. Okamura, S. Akiyama, H. Namatame, and M. Taniguchi, J. Electron Spectrosc. Relate. Phenom. **88-91**, 1027 (1998).
[24] F. J. Himpsel, Surf. Sci. Rep. **12**, 1 (1990).
[25] H. Liebl, Optik **53**, 69 (1979).
[26] H. Liebl, Nucl. Instrum. Meth. A **292**, 537 (1990).
[27] J. T. Yates Jr., in: *Experimental Innovations in Surface Science* (Springer, New York, 1998), p. 288.
[28] J. T. Yates Jr., in: *Experimental Innovations in Surface Science* (Springer, New York, 1998), p. 304.
[29] J. A. R. Samson, *Techniques of Vacuum Ultraviolet Spectroscopy* (John Wiley and Sons, New York, London, Sydney, 1969)
[30] W. Trott, C. Blais, and E. Walters, J. Chem. Phys. **69**, 3150 (1978).
[31] V. H. Dibeler, J. A. Walker, K. E. McCullooh, and H. M. Rosenstock, Int. J. Mass Spectrom. Ion Phys. **7**, 209 (1971).
[32] V. Dose, W. Altmann, A. Goldmann, U. Kolac, and J. Rogozik, Phys. Rev. Lett. **52**, 1919 (1984).
[33] D. Straub and F. J. Himpsel, Phys. Rev. Lett. **52**, 1922 (1984).
[34] U. Höfer, I. L. Shumay, Ch. Reuß, U. Thomann, W. Wallauer, and Th. Fauster, Science **277**, 1480 (1997).
[35] Th. Fauster and W. Steinmann, in: *Electromagnetic Waves: Recent Developments in Research, Vol. 2: Photonic Probes of Surfaces*, ed. by P. Halevi (Elsevier, Amsterdam, 1995), p. 347.
[36] F. Passek and M. Donath, Phys. Rev. Lett. **69**, 1101 (1992).